






# Epigenetic Suppression of Interferon Lambda Receptor Expression Leads to Enhanced Human Norovirus Replication *In Vitro*

Sabastine E. Arthur,<sup>a</sup>  Frédéric Sorgeloos,<sup>a</sup>  Myra Hosmillo,<sup>a</sup>  Ian G. Goodfellow<sup>a</sup>

<sup>a</sup>Division of Virology, Department of Pathology, Addenbrooke's Hospital, University of Cambridge, Cambridge, United Kingdom

**ABSTRACT** Human norovirus (HuNoV) is the main cause of gastroenteritis worldwide, yet no therapeutics are currently available. Here, we utilize a human norovirus replicon in human gastric tumor (HGT) cells to identify host factors involved in promoting or inhibiting HuNoV replication. We observed that an interferon (IFN)-cured population of replicon-harboring HGT cells (HGT-Cured) was enhanced in their ability to replicate transfected HuNoV RNA compared to parental HGT cells, suggesting that differential gene expression in HGT-Cured cells created an environment favoring norovirus replication. Microarrays were used to identify genes differentially regulated in HGT-NV and HGT-Cured compared to parental cells. We found that IFN lambda receptor (IFNLR1) expression was highly reduced in HGT-NV and HGT-Cured cells. While all three cell lines responded to exogenous IFN- $\beta$  by inducing interferon-stimulated genes, HGT-NV and HGT-Cured cells failed to respond to exogenous IFN- $\lambda$ . Methylation-sensitive PCR showed that an increased methylation of the IFNLR1 promoter and inhibition of DNA methyltransferase activity partially reactivated IFNLR1 expression in HGT-NV and HGT-Cured cells, indicating that host adaptation occurred via epigenetic reprogramming. Moreover, IFNLR1 ectopic expression rescued response to IFN- $\lambda$  and restricted HuNoV replication in HGT-NV cells. We conclude that type III IFN is important in inhibiting HuNoV replication *in vitro* and that the loss of IFNLR1 enhances replication of HuNoV. This study unravels for the first time epigenetic reprogramming of the interferon lambda receptor as a new mechanism of cellular adaptation during long-term RNA virus replication and shows that an endogenous level of interferon lambda signaling is able to control human norovirus replication.

**IMPORTANCE** Noroviruses are one of the most widespread causes of gastroenteritis, yet no suitable therapeutics are available for their control. Moreover, to date, knowledge of the precise cellular processes that control the replication of the human norovirus remains ill defined. Recent work has highlighted the importance of type III interferon (IFN) responses in the restriction of viruses that infect the intestine. Here, we analyzed the adaptive changes required to support long-term replication of noroviruses in cell culture and found that the receptor for type III IFN is decreased in its expression. We confirmed that this decreased expression was driven by epigenetic modifications and that cells lacking the type III IFN receptor are more permissive for norovirus replication. This work provides new insights into key host-virus interactions required for the control of noroviruses and opens potential novel avenues for their therapeutic control.

**KEYWORDS** DNA methylation, human norovirus replicon, epigenetic reprogramming, interferon lambda receptor, microarrays

**W**ith the introduction of the rotavirus vaccine, human norovirus (HuNoV) is now the main etiologic agent responsible for gastroenteritis worldwide (1–4). The disease, characterized by diarrhea, nausea, and vomiting, is generally self-limiting in

**Citation** Arthur SE, Sorgeloos F, Hosmillo M, Goodfellow IG. 2019. Epigenetic suppression of interferon lambda receptor expression leads to enhanced human norovirus replication *in vitro*. *mBio* 10:e02155-19. <https://doi.org/10.1128/mBio.02155-19>.

**Editor** Stacey Schultz-Cherry, St. Jude Children's Research Hospital

**Copyright** © 2019 Arthur et al. This is an open-access article distributed under the terms of the [Creative Commons Attribution 4.0 International license](https://creativecommons.org/licenses/by/4.0/).

Address correspondence to Frédéric Sorgeloos, frederic.sorgeloos@gmail.com, or Ian G. Goodfellow, ig299@cam.ac.uk.

S.E.A. and F.S. contributed equally to this work.

**Received** 23 August 2019

**Accepted** 26 August 2019

**Published** 1 October 2019

healthy adults. However, in immunocompromised, elderly patients and young children under the age of five, the disease can become chronic and sometimes lead to death, mostly due to dehydration (5–9). Despite this and the profound economic burden of the disease (10), there are no therapeutics or licensed vaccines available.

Until the advent of the B lymphocyte-based and stem cell-derived human intestinal enteroid culture systems (11, 12), HuNoV research has been hampered by the lack of cell culture and small animal models recapitulating noroviral infection and pathogenesis. However, limitations in robustness, cost, and labor-intensiveness associated with both methods show that advances in HuNoV research still rely on the well-established murine norovirus (MNV) infection model and norovirus replicon systems (13, 14). These systems have been used to identify key host factors that impact the life cycle of HuNoV, reviewed by Thorne and Goodfellow (15).

While type I interferons (IFN- $\alpha/\beta$ ) were discovered more than a half century ago (16), type III interferons (IFN- $\lambda$ ) were discovered only a little over a decade ago (17, 18). Although the two cytokine families possess similar functions, a few but crucial differences exist in their biology. Notably, both cytokines signal through distinct heterodimeric receptors with type I IFN signaling through the interferon alpha/beta receptor (IFNAR), composed of the IFNAR1 and IFNAR2 subunits, and type III IFN signaling through the interferon lambda receptor (IFNLR), which consists of the interferon lambda receptor 1 (IFNLR1) and interleukin 10 receptor beta (IL10RB) subunits. Unlike the type I IFN receptor that is expressed on most cell types, expression of the IFNLR1 subunit is restricted to cells of the mucosal epithelium, neutrophils, and human hepatocytes (19–21). Although the immune cells of the blood were also shown to express the IFNLR1 subunit, the receptor has been reported to lack the ability to respond to IFN- $\lambda$  (22).

Expression of type I and III interferons is regulated at the transcriptional level and relies on the recognition of conserved pathogen-associated molecular patterns (PAMPs). Detection of these molecular signatures by extracellular and intracellular pattern recognition receptors triggers the coordinated activation of distinct signaling pathways responsible for the activation of IRF3/7 and NF- $\kappa$ B transcription factors that are required for IFN gene transcription. Secreted IFN- $\lambda$  then binds to the IFNLR and is thought to activate the Janus kinase 1 and tyrosine kinase 2. Subsequently, recruited signal transducer and activator of transcription 1 (STAT1) and STAT2 are activated through phosphorylation, leading to the expression of IFN-stimulated genes (ISGs), some of which have direct antiviral activities (23). Interferon lambdas are important players in both innate and adaptive immunity and have profound antiviral effects on a variety of viruses (24–28). Expression of IFNLR1 on epithelial cells of the small intestine and colon was shown to be important in IFN- $\lambda$ -mediated antiviral activity against persistent MNV and reovirus infection *in vivo* (29). Treatment of persistently infected mice lacking the adaptive immune response (Rag1<sup>-/-</sup>) with IFN- $\lambda$  abolished viral replication, suggesting that IFN- $\lambda$  can cure persistent MNV infection in the absence of adaptive immunity and that this ability requires the expression of IFNLR1 (30). In line with this, the effect of antibiotics that inhibit persistent MNV infection in the gut has also been shown to be dependent on IFNLR1 expression as well as IRF3 and STAT1 transcription factors (31). It was observed that AG129 sentinel mice lacking the ability to respond to both IFN- $\alpha/\beta$  and IFN- $\gamma$  housed together with MNV-infected mice developed a diarrhea-associated MNV infection. Overexpression of IFN- $\lambda$  in sentinel mice upregulated ISG expression, inhibited MNV replication in the small intestine, and prevented them from being infected when cohoused with MNV-infected mice (32). While numerous studies on the related murine norovirus have been published, there is a paucity of data on its human counterpart. It has been recently suggested that while the human norovirus replication is hampered by type I and III interferon treatment (33, 34), HuNoV RNA replication itself seems not to induce innate immune responses, implying that endogenous IFN response may have a limited role in controlling HuNoV infection (33). Thus, the magnitude and importance of the innate immune responses in modulating the HuNoV replication are unclear. In this study, we sought to pinpoint

cellular pathways altered during HuNoV replication. Using microarrays on replicon-harboring epithelial cells, we identified transcriptome signatures consistent with an activation of autonomous immune responses. Consistent with this, we found a strong downregulation of the IFN lambda receptor (IFNLR1) expression, rendering cells insensitive to exogenous IFN- $\lambda$ . Mechanistically, epigenetic studies revealed an increased methylation of the IFNLR1 promoter, strongly suggesting an involvement of type III interferons in controlling HuNoV replication.

(This article was submitted to an online preprint archive [35].)

## RESULTS

**Generation and characterization of human cell lines bearing stable human norovirus replicons.** To understand the influence of viral and host factors involved in HuNoV replication, we sought to generate several human cell lines stably replicating HuNoV RNA. To this end, BHK-21 cells were transfected with capped Norwalk replicon RNA harboring a neomycin selection marker (14) and subjected to G418 selection 48 h after transfection (Fig. 1A). Although the vast majority of the cells died within 1 week, individual cell colonies were observed and subjected to limiting dilution. A single high-expressing clone was selected and expanded to generate stable replicon-containing BHK-21 cells (BHK-NV). VPg-linked RNA extracted from these cells was transfected into HGT cells, a cell line of epithelial origin which was subsequently selected on the basis of the cells' G418 resistance in order to generate human norovirus replicon cells (HGT-NV). These HGT-NV cells were either collected as a population or subjected to limiting dilution to produce HGT-NV cell clones. The HGT-NV population was further passaged 16 times in the presence of IFN- $\alpha$  at a concentration of 1,000 U/ml in the absence of G418 selection over an 8-week period, leading to the generation of HGT-Cured cells. These cells were subsequently cultured in the presence of G418 to observe their loss of resistance to G418, confirming the complete elimination of the replicon. Detection of HuNoV RNA by RT-qPCR analysis confirmed the presence of noroviral genomes in HGT-NV cells that were absent from HGT-Cured or parental HGT cells used as control (Fig. 1B). To confirm the presence of authentic steady-state replication of Norwalk virus RNA, cells were subjected to immunofluorescence analysis using monoclonal antibodies directed against double-stranded RNA (dsRNA), a by-product assumed to be universally generated during viral replication (36, 37). As shown in Fig. 1C, punctate structures reminiscent of replication complexes were identified in HGT-NV cells while no signal above background levels was detected in HGT-Cured or in parental cell lines. Taken together, these results suggest that HuNoV VPg-linked RNA successfully replicates in HGT cells and displays all the characteristics of a replication-competent RNA.

**Cured population of HGT-NV cells demonstrates enhanced HuNoV replication.** Stable viral RNA replication under drug-mediated selection leads to an environment where, on the one hand, host cells face the selective pressure of the drug and, on the other hand, replicating RNA faces innate cellular responses aimed at inhibiting replication. This results in the establishment of a metastable equilibrium prone to adaptation from both cells and the replicating viral RNA. To test for the appearance of such adaptive mutation(s) in the replicon, VPg-linked RNA was extracted from BHK-NV and HGT-NV cells and subjected to consensus genome sequencing. Sequence analysis revealed that viral RNA originating from both BHK-NV and HGT-NV cells underwent many synonymous and nonsynonymous genomic changes, suggesting the potential adaptation of HuNoV RNA to specific cellular environments (see Table S1 in the supplemental material). To test specifically for host cell adaptation, wild-type VPg-linked RNA extracted from BHK-NV cells was retransfected in both HGT and HGT-Cured cell lines that were subsequently selected for 5 days with G418. As shown in Fig. 2A, HGT-Cured cells gave rise to a greater number of stable replicon colonies than parental HGT cells. To quantitatively confirm this observation, each cell line was transfected with wild-type VPg-linked RNA replicon and cells were harvested at various time points for RNA extraction and viral RNA quantification (Fig. 2B). From 5 days posttransfection, the

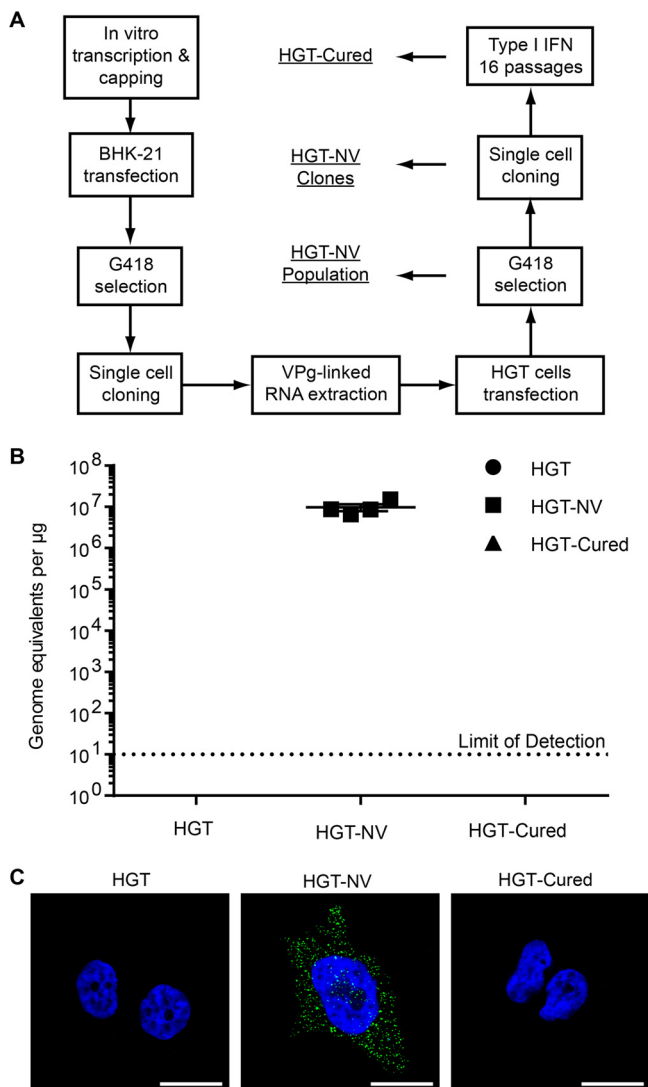


**FIG 1** Generation and characterization of stable HuNoV replicons in HGT cell lines. (A) Diagram showing the steps used to generate the various cell lines carrying human norovirus replicons and their IFN-cured counterparts. (B) Total cellular RNA was extracted from each cell line, and viral RNA was quantified by RT-qPCR. Viral RNA copy numbers were normalized to the total input RNA and expressed as genome equivalents per microgram of input RNA. The error bars represent the standard deviation determined from four biological replicates. Viral RNA copy numbers were below the limit of detection in both HGT and HGT-Cured cells. The dotted line represents the low limit of detection. (C) Detection of viral replication complexes by confocal imaging. Representative merged confocal micrographs showing the detection of dsRNA (green) in indicated cell lines. Nuclei were stained with DAPI (blue). Bars, 20  $\mu\text{m}$ .

levels of Norwalk virus replicon RNA were significantly higher in HGT-Cured cells than HGT cells. Noroviral RNA levels further increased at day 6 to yield a 15-fold difference between HGT-Cured and HGT cells. Quantification of transfected VPg-linked viral RNA at 6 h posttransfection revealed similar levels in HGT and HGT-Cured cells, suggesting that IFN treatment did not alter the ability of HGT-Cured cells to be transfected (data not shown). We thus concluded that HGT-Cured cells possess a greater degree of permissiveness to viral replication than parental HGT cells.

**An alteration in cellular environment is responsible for enhanced viral replication in HGT-Cured cells.** Increased replication of HuNoV VPg-linked RNA in HGT-Cured cells suggests that these cells provide a better cellular environment than that of parental HGT cells. To get insights into the mechanism of this cell-derived HuNoV replicon permissiveness, genome-wide expression profiles from HGT, HGT-NV, and

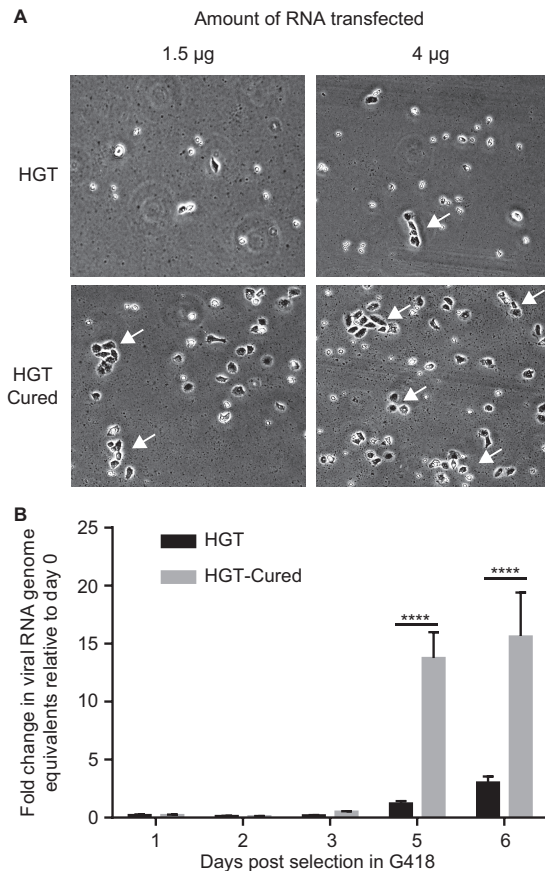


**FIG 2** HGT-Cured cells demonstrate enhanced HuNoV replication. (A) HGT and HGT-Cured cells were transfected with VPg-linked replicon RNA. After 5 days of selection with G418 at a concentration of 0.5 mg/ml, cellular morphology was analyzed by light microscopy. (B) Cells transfected with VPg-linked RNA were harvested at various time points posttransfection for total RNA extraction, and viral RNA was quantified by RT-qPCR. Viral RNA levels were determined by comparison to a standard curve and normalized to the RNA input. The data are presented as mean and standard deviation from three replicates. Indicated values are expressed as fold change in genome equivalents normalized to viral RNA levels at 6 h posttransfection to control for transfection efficiency. Unpaired two-tailed Student's *t* test was used to evaluate the statistical significance.

HGT-Cured cell lines were quantified using Illumina BeadChip microarrays (Tables S2 and S3). We first compared the gene expression profiles of HGT-NV cells relative to their HGT controls. As seen in Fig. 3A, more than 2,000 genes (HGT-NV versus HGT, 2,074; HGT-Cured versus HGT, 858) were identified for which mRNA expression was significantly modified at a false-discovery rate (FDR) lower than 0.01. Of these, a minority of 151 genes had expression changes in either direction greater than 2-fold, suggesting that HuNoV replication has a marginal effect on the whole transcriptional landscape of replicon-harboring cells. Using the same criteria, comparison of gene expression profiles between HGT cells and HGT-Cured cells led to identification of 101 genes for which expression was differentially regulated between the two cell lines (Tables S4 and S5). To confirm these observations and to probe for the accuracy of gene expression measured by microarray analysis, we first compared expression changes obtained by microarrays with that measured by RT-qPCR analysis. To this end, 10 genes differentially regulated across conditions and spanning a wide range of fold changes were chosen for RT-qPCR validation (Fig. 3B). Globally, we observed a high correlation between the two techniques, with Pearson's correlation coefficients ranging from 0.90 to 0.95. Direct comparison of raw microarray signal intensities with differences in cycle threshold ( $\Delta C_T$ ) obtained by real-time PCR displayed the same trends, suggesting that similar fold changes were primarily the consequence of gene expression differences and were not

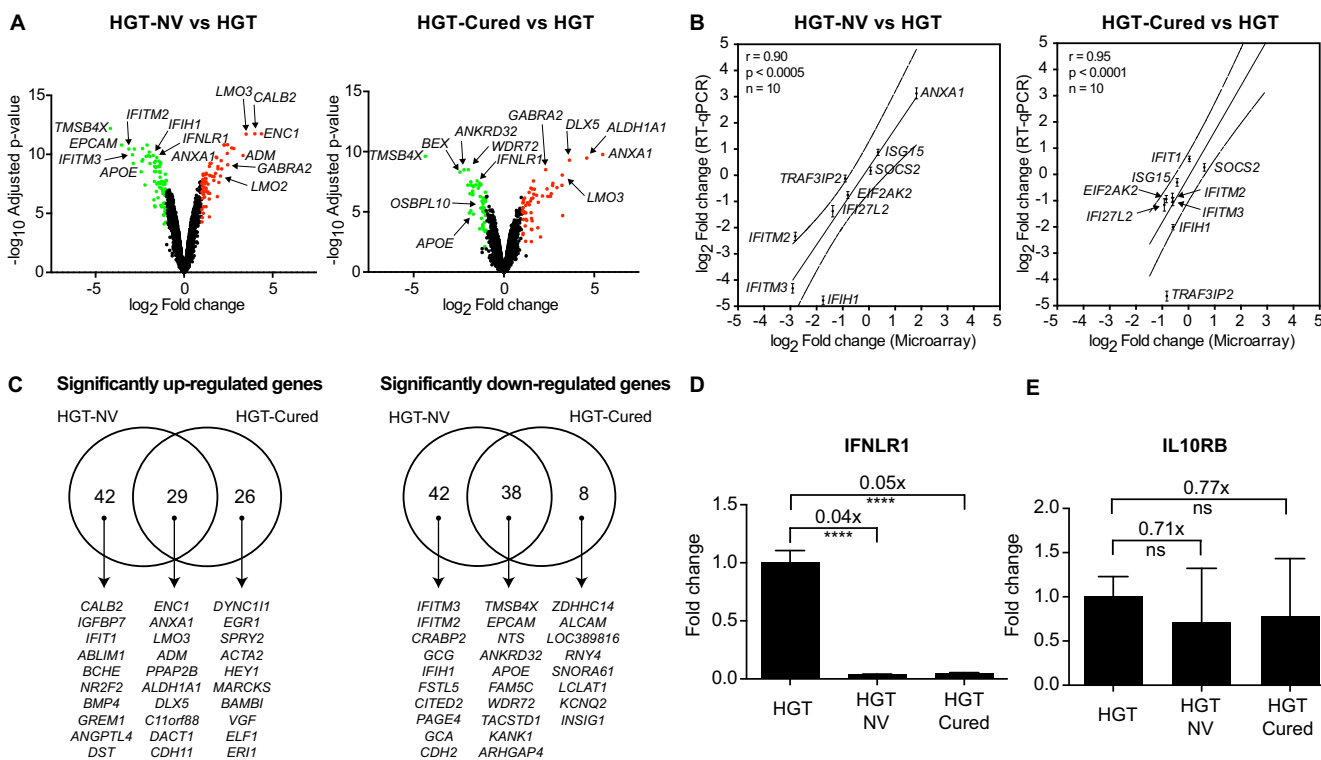


**FIG 3** Microarray analysis and validation of differentially regulated genes between HGT-NV, HGT-Cured, and parental HGT cells. (A) Volcano plots of differentially expressed genes from microarray analysis comparing gene expression in HGT-NV or HGT-Cured cells with that in parental HGT cells. Significantly up- or downregulated genes ( $FDR < 0.01$  and  $|\log_2 \text{fold change}| \geq 1$ ) are represented in red or green, respectively. (B) Fold change correlation between microarray analysis and quantitative real-time PCR (RT-qPCR). Scatter plots comparing  $\log_2$  fold changes of selected genes measured by microarray analysis and RT-qPCR in HGT-NV or HGT-Cured cells compared to parental HGT cells. Error bars represent the standard deviation from biological quadruplicate experiments analyzed in triplicate reactions. The Pearson correlation coefficient ( $r$ ) and the number of pairs analyzed ( $n$ ) are indicated on each graph. Dotted lines illustrate the 95% confidence interval of the linear regression. (C) Venn diagrams representing the overlap of significantly up- and downregulated genes between HGT-NV or HGT-Cured cells and parental HGT cells. The top 10 genes within each category are shown. (D and E) IFNLR1 (D) but not IL10RB (E) gene expression is downregulated in HGT-NV and HGT-Cured cells. Changes in gene expression of IFNLR1 and IL10RB mRNA levels were normalized to  $\beta$ -actin levels and calculated using the  $\Delta\Delta C_T$  method. Relative expression was determined from one experiment performed in biological triplicate and compared to the expression levels measured in HGT control. Statistical significance was determined using the unpaired  $t$  test. Error bars represent the standard deviation between biological replicates. ns, not significant.

an artifact resulting from different gene normalization techniques. Differential gene expression at the protein level of selected genes was further confirmed by Western blot analysis (Fig. S1A and B). Taken together, these data extensively confirm the reliability of gene expression measurements by microarray analysis.

The number of genes showing similar regulation between HGT-NV and HGT-Cured is surprisingly high and likely reflects cellular long-term adaption to replicating RNA (GO term enrichment analysis did not reveal specific pathway enrichment in this gene set). Remarkably, we observed an opposite regulation of several interferon-stimulated genes (ISGs) when comparing the HGT-NV transcriptional landscape with that of parental HGT cells (Fig. 3C and Table S4). While genes coding for IFITM2, IFITM3, IFIH1, and IFI27L2 were downregulated, IFIT1 and IFIT2 genes were significantly upregulated in HGT-NV cells. Expression of IFIT1 and IFIT2 proteins is known to be IRF3 dependent (38, 39), while expression of IFITM and IFIH1 genes was shown to be mediated by ISRE binding (40, 41); this suggests that while HuNoV replication induces IRF3-dependent immune responses, activation of ISRE-dependent genes located downstream in the interferon signaling pathway is inhibited. In line with this observation, microarray analysis identified a statistically significant downregulation of the type III interferon receptor (IFNLR1) expression in HGT-NV and HGT-Cured cells when both were compared to HGT cells. To confirm and extend this observation, we compared IFNLR1 and IL10RB gene expression by quantitative RT-PCR. Remarkably, we found more than 20-fold decrease in IFNLR1 expression when parental HGT cells were compared to HGT-NV or HGT-Cured

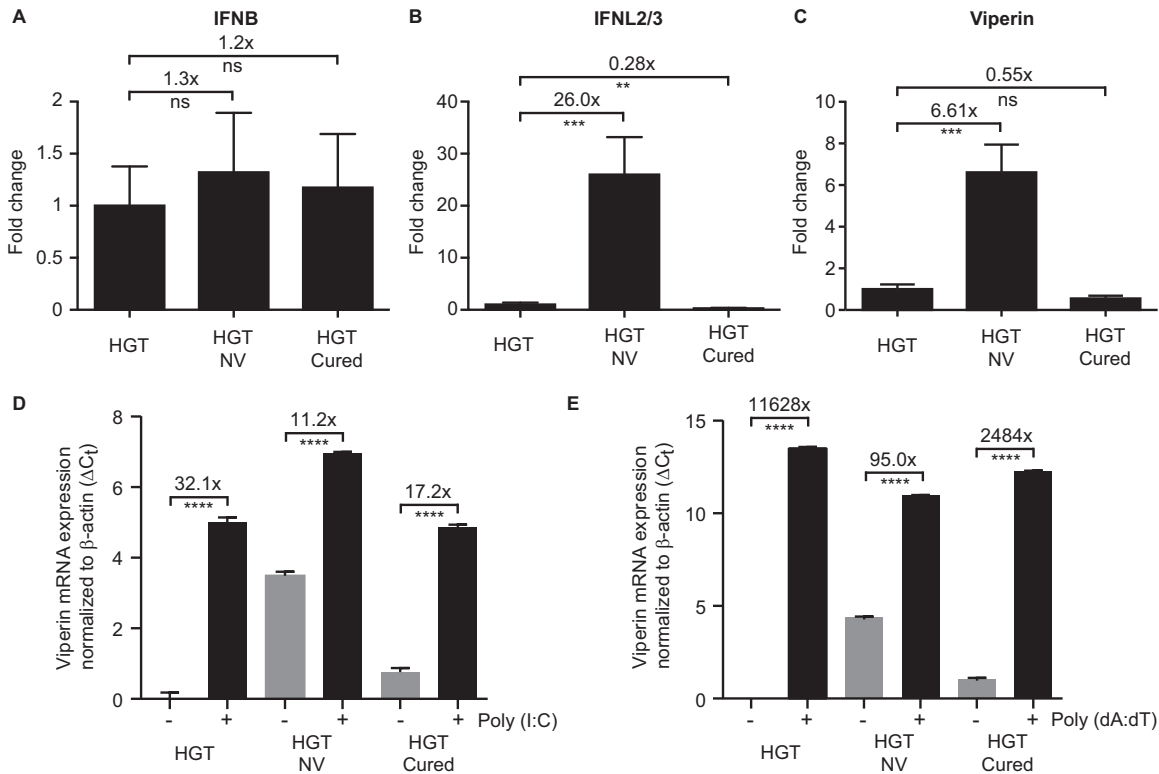


**FIG 4** Innate immune responses to RNA and DNA PAMPs are functional. (A to C) Quantitative expression analysis of IFNB (A), IFNL2/3 (B), and viperin (C) mRNAs. Relative gene expression was determined from one experiment performed in biological triplicate and compared to the expression levels measured in HGT cells. Statistical significance was determined using the unpaired *t* test. Error bars represent the standard deviation between biological replicates. (D and E) Cells were transfected with poly(I:C) (D) or poly(dA:dT) (E), and total RNA was harvested 8 h posttransfection for quantification of viperin mRNA levels by RT-qPCR. Viperin mRNA levels were expressed as differences of cycle threshold ( $C_t$ ) of viperin relative to the  $C_t$  of beta-actin. The error bars represent standard deviation, determined from the result of three replicates.

cells. In contrast, no significant difference was observed when IL10RB gene expression was measured (Fig. 3D and E).

**Sensing of cytosolic RNA and DNA PAMPs by the innate immune system is functional.** Downregulation of the type III interferon receptor expression suggests that lambda interferons are preferentially expressed in HGT-NV cells, providing a basis for selection of IFNL1 downregulation. To probe this hypothesis, we measured both type I and type III interferon expression levels by quantitative RT-qPCR. While no difference in IFNB expression was detected between cell lines (Fig. 4A), a significant 26-fold-higher expression of interferon lambda 2/3 was detected in cells replicating the noroviral RNA, suggesting that viral RNA is indeed readily detected in HGT-NV cells (Fig. 4B). In line with this observation, we found a more than 6-fold increase in viperin expression when HGT-NV cells were compared to HGT parental cells. To examine whether HGT-NV and HGT-Cured cells were able to detect and mount an innate immune response against cytosolic PAMPs, poly(I:C) and poly(dA:dT) were transfected in the various HGT-derived cell lines and viperin expression levels were measured by RT-qPCR (Fig. 4D and E). Although the cell lines exhibited upregulation of viperin mRNA to various extents, a significant increase of viperin expression above basal levels was detected in all the three cell lines in response to both poly(I:C) and poly(dA:dT). Given that the overall levels of viperin following treatment were comparable across the three cell lines, evident by the relative ratio with respect to  $\beta$ -actin, we concluded that PAMP sensing and downstream signaling pathways are functional in these cell lines.

**The ability to respond to type III but not type I IFN in HGT-NV and HGT-Cured cells is debilitated.** We next investigated the ability of type I and type III interferons to elicit ISG induction. To this end, cells were incubated with human IFN- $\beta$  or IFN- $\lambda$ 2 for

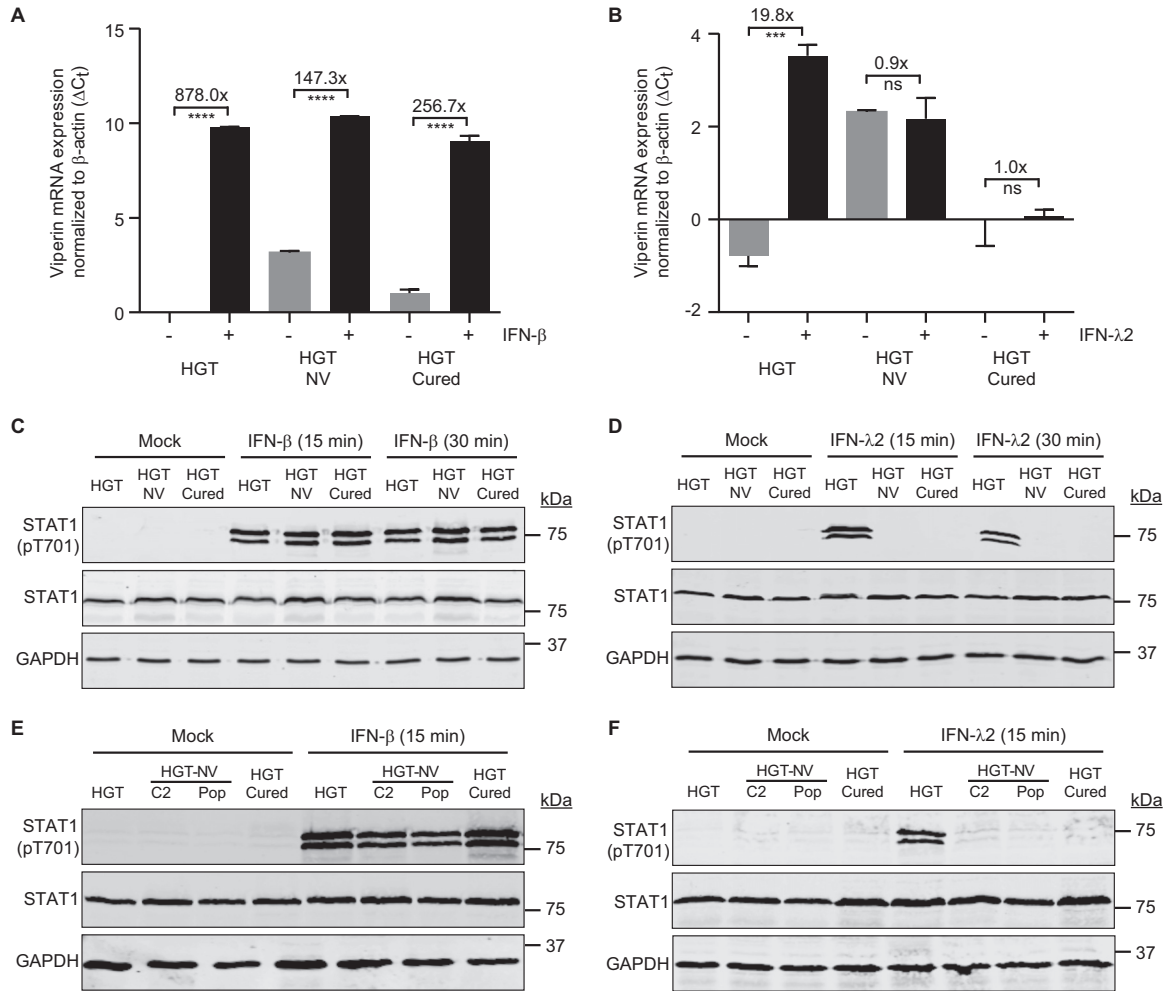


**FIG 5** The ability to respond to type III but not type I IFN is debilitated in HGT-NV and HGT-Cured cells. (A and B) Cells were treated with type I (IFN- $\beta$ ) (A) or type III interferon (IFN- $\lambda$ 2) (B), incubated overnight, and harvested for total RNA extraction and quantification of viperin mRNA levels by RT-qPCR. Viperin mRNA expression levels were expressed as differences of cycle threshold ( $C_T$ ) of viperin from the  $C_T$  of beta-actin. The error bars represent the standard deviation, determined from the result of three replicates. (C to F) Western blot analysis showing STAT1 phosphorylation after stimulation with type I and type III interferons in HGT, HGT-NV, and HGT-Cured cell lines (C and E). HGT-NV clone 2 (C2) and populations of cells (Pop) were included in the experiment (D and F). Glyceraldehyde-3-phosphate dehydrogenase (GAPDH) was used as a loading control.

16 h and viperin expression levels were measured by RT-qPCR. We observed that viperin mRNA was readily induced in all three cell lines in response to exogenous type I IFN (IFN- $\beta$ ) treatment (Fig. 5A). However, whereas HGT cells responded to exogenous type III IFN (IFN- $\lambda$ 2) treatment, HGT-NV and HGT-Cured cells did not (Fig. 5B). To test whether the absence of ISG expression is linked to a defect of STAT1 phosphorylation in response to type I or type III interferons, cells were incubated with either recombinant IFN- $\beta$  or IFN- $\lambda$ 2 and STAT1 phosphorylation status was analyzed by Western blotting using anti-STAT1 phosphospecific antibodies. We observed that although STAT1 was phosphorylated in all cell lines following IFN- $\beta$  treatment (Fig. 5C), no STAT1 phosphorylation was detected in HGT-NV and HGT-Cured cells following IFN- $\lambda$ 2 treatment (Fig. 5D). To ensure that the absence of STAT1 phosphorylation in HGT-NV cells is not due to a potential clonal effect, different clones as well as a population of the HGT-NV cells were included in the experiment. Similarly, the clones represented here by clone 2 (C2) and the polyclonal cell population responded to IFN- $\beta$  but not to IFN- $\lambda$ 2 (Fig. 5E and F). Taken together, these results indicate that signal transduction induced by type I IFN is intact while STAT1 phosphorylation induced in response to lambda interferon is inhibited in HGT cells that sustained HuNoV replication.



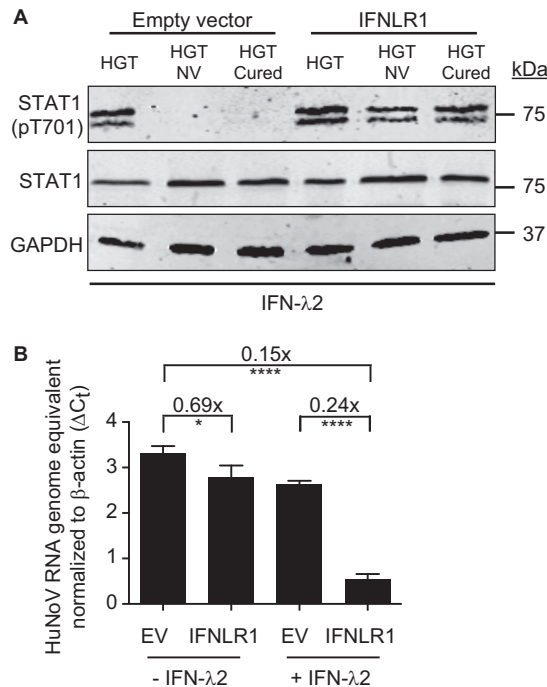


**FIG 6** Overexpression of IFNLR1 in HGT-NV and HGT-Cured cells rescues the ability to respond to type III IFN and negatively impacts HuNoV replication. (A) HGT, HGT-NV, and HGT-Cured were transfected with IFNLR1-expressing plasmid, and STAT1 phosphorylation was measured in whole-cell lysate by Western blotting after incubating cells with type III IFN for 15 min. STAT1 was used as a positive control, and GAPDH was used as the loading control. (B) HGT-NV cells were transfected with IFNLR1-expressing plasmid or an empty vector. After 2 days, cells were stimulated for 96 h with type III interferon or were left untreated. Total cellular RNA was extracted, and viral RNA was quantified by RT-qPCR. HuNoV replication levels were expressed as differences of cycle threshold ( $C_T$ ) of HuNoV from the  $C_T$  of beta-actin. The error bars represent the standard deviation, determined from the result of three replicates. Statistical significance was determined using the unpaired *t* test.

**IFNLR1 overexpression rescues STAT1 phosphorylation in response to IFN lambda and decreases viral replication.** To directly test whether the downregulation of IFNLR1 expression measured in HGT-NV and HGT-Cured cells is responsible for their unresponsiveness to lambda interferon, cells were transfected with an IFNLR1-expressing plasmid and stimulated with IFN-λ2 the day after. We observed that IFNLR1 expression rescued STAT1 phosphorylation in response to interferon lambda, suggesting that IFNLR1 downregulation in HGT-NV and HGT-Cured cells is responsible for IFN-λ insensitivity (Fig. 6A). In addition, this experiment shows that the JAK-STAT signaling cascade comprising JAK1, Tyk2, and possibly JAK2 (42) is functional and leads to the phosphorylation of STAT1. We next investigated whether transient IFNLR1 overexpression negatively impacts HuNoV replication. To this end, HGT-NV cells were transfected with an IFNLR1-expressing plasmid and HuNoV replication was monitored by quantitative RT-PCR. In the absence of IFN-λ2, we observed a modest but statistically significant reduction of viral replication when IFNLR1-transfected cells were compared to cells transfected with the empty vector (Fig. 6B). This reduction of HuNoV replication greatly increased when cells were stimulated with IFN-λ2, suggesting that IFNLR1 downregulation in HGT-NV cells is prominently responsible for their ability to support enhanced viral replication.

**Inactivation of interferon type I and III receptors increases HuNoV replication in epithelial cells.** To directly test the influence of type I and type III IFNs on HuNoV replication, HGT cell lines deficient either for the interferon alpha/beta receptor IFNAR1 or for the interferon lambda receptor IFNLR1 were generated using CRISPR/Cas9-mediated genome editing. To this end, parental HGT cells were transduced with lentiviruses expressing IFNAR1 or IFNLR1 single guide RNAs and clonally selected in the

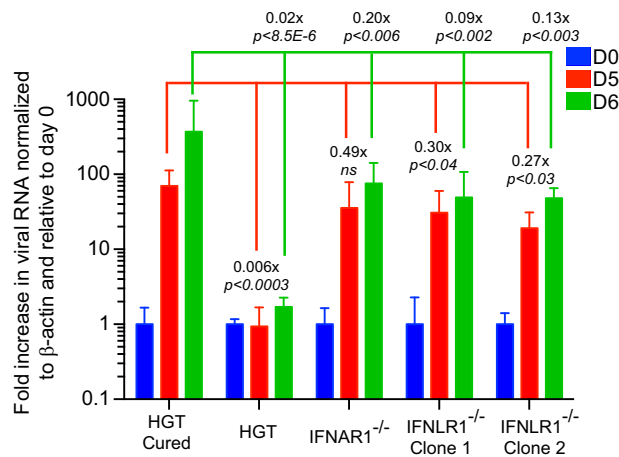


**FIG 7** Genetic ablation of IFNAR1 and IFNLR1 interferon receptors promotes HuNoV replication. Parental HGT, IFNAR1, and IFNLR1 knockout cells were transfected with VPg-linked replicon RNA and submitted to G418 selection. Total cellular RNA was harvested at various time points posttransfection, and viral RNA was quantified by RT-qPCR. Relative viral replication was determined from one experiment performed in biological triplicate and compared to the replication levels measured in HGT-Cured cells at day 0. Statistical significance was determined using the unpaired *t* test. Error bars represent the standard deviation between biological replicates.

presence of puromycin. Individual clones were screened for gene inactivation by IFN- $\beta$  or IFN- $\lambda$ 2 challenge followed by analysis of STAT1 phosphorylation by Western blotting and viperin induction by RT-qPCR (Fig. S2A and B). VPg-linked viral RNA was then transfected, and cells were selected in the presence of 0.5 mg/ml G418 for up to 6 days. Relative to day 0 taken as reference, we observed a significant increase in genomic viral RNA in all cell lines with the exception of parental HGT cells, corroborating the antiviral activity of both type I and type III IFNs on HuNoV replication (Fig. 7). Similarly, an increased ability of modified cell lines to promote colony formation induced by the HuNoV replicon was observed (data not shown).

**The IFNLR1 promoter is methylated in HGT-NV and HGT-Cured cells.** The dimeric interferon lambda receptor consists of the ubiquitously expressed IL10RB chain subunit and the interferon lambda-specific chain IFNLR1, whose expression is limited to cells of epithelial origin (20). Cell-type-specific expression of the IFNLR1 subunit was later shown to be inversely correlated with the methylation of its promoter (43). To examine whether viral replication induced, or led to the selection of, alterations of IFNLR1 gene expression through epigenetic modifications, cells were incubated in the presence of 5-aza-2'-deoxycytidine (5azadC), a deoxynucleoside analogue that strongly inhibits DNA methyltransferase (DNMT) activity. As shown in Fig. 8A, we observed a significant 6-fold increase of IFNLR1 mRNA levels in HGT-NV cells compared to cells incubated with the vehicle only. A statistically significant increase in IFNLR1 gene expression was also observed in the case of HGT-Cured cells but to a lower extent (2.8-fold). In contrast, no change in IL10RB expression was detected when the same cells were incubated with 5azadC (Fig. 8B). In addition, incubation in the presence of the histone deacetylase (HDAC) inhibitor MS-275 alone or in combination with 5azadC did not result in increased IFNLR1 or IL10RB expression, suggesting that replicating HuNoV did not modify the chromatin structure of these genes. We next assessed the methylation status of the IFNLR1 promoter by methylation-sensitive PCR using McrBC, a GTP-dependent endonuclease that restricts DNA fragments containing methylated cytosines. To this end, genomic DNA extracted from HGT, HGT-NV, and HGT-Cured cell lines was digested with McrBC and digestion products were amplified by PCR. The amplicon, which spans a CpG island from -211 to +216 bp relative to the IFNLR1 transcription start site, is located in a promoter region previously shown to be methylated in cells of nonepithelial origin (43). Interestingly, we observed less PCR amplification in McrBC-digested samples originating from HGT-NV or HGT-Cured cells than in

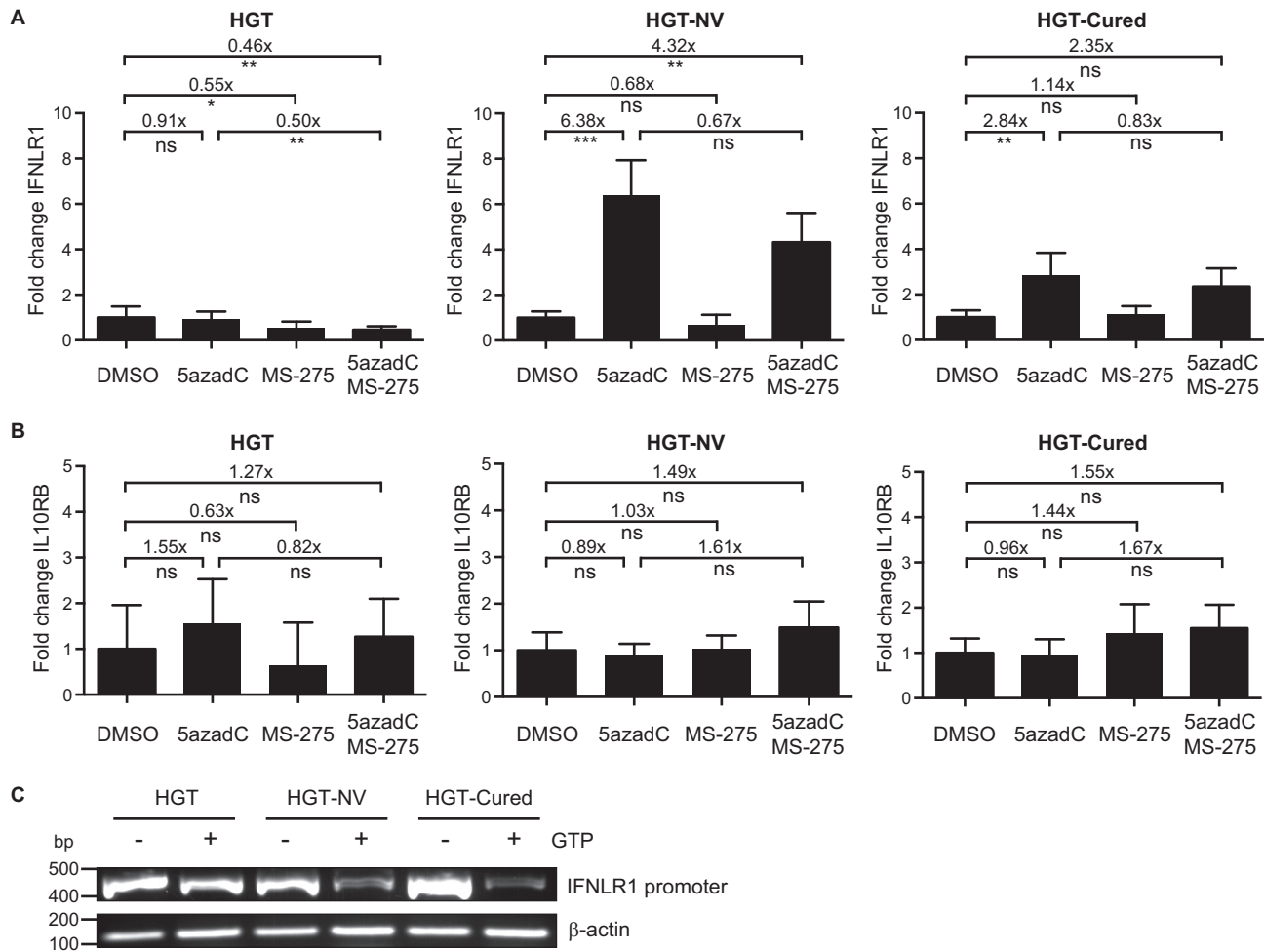


**FIG 8** IFNL1 promoter is methylated during long-term HuNoV replication. (A and B) HGT, HGT-NV, and HGT-Cured cells were incubated in the presence of 10  $\mu$ M 5azadC for 72 h or left untreated. When indicated, cells were also incubated in the presence of 1  $\mu$ M MS-275 in the last 24 h. Total cell RNA was extracted, and IFNL1 (A) and IL10RB (B) expression levels were measured by RT-qPCR. Relative gene expression was determined from one experiment performed in biological triplicate and compared to the expression levels measured in corresponding vehicle-treated cells. Statistical significance was determined using the unpaired *t* test. Error bars represent the standard deviation between biological replicates. DMSO, dimethyl sulfoxide. (C) Genomic DNA extracted from HGT, HGT-NV, and HGT-Cured cells was digested with MspI in the absence or presence of GTP. Digestion products were subsequently subjected to PCR amplification analysis using primers specific for the IFNL1 promoter. Beta-actin PCR products were used as loading control.

parental HGT cells, confirming a greater degree of methylation of their IFNL1 promoters (Fig. 8C). In addition, this experiment shows that the same region of the IFNL1 promoter is methylated in both physiological and pathological processes, suggesting that epigenetic control is the main mechanism of *IFNL1* gene expression regulation. Taken together, these results suggest that the replication of HuNoV in HGT epithelial cells induces a long-term transcriptional silencing of the *IFNL1* gene through the methylation of its promoter.

## DISCUSSION

The purpose of this study was to compare genome-wide transcriptional responses of epithelial cells supporting autonomous HuNoV replication with those elicited by IFN-cured derivatives showing increased viral replication abilities. We found that the interferon lambda receptor is downregulated in cells that sustained HuNoV replication. Mechanistically, this downregulation of IFNL1 was mediated by gene methylation as shown by methylation-sensitive PCR and by the fact that treatment with 5azadC, a DNA methyltransferase inhibitor, rescued the phenotype. This suggests that the lambda IFN pathway is a key constituent of the innate intrinsic defense against human norovirus

and shows that an endogenous IFN lambda signaling activity is able to modulate the replication of the virus.

Influence of lambda interferons on murine noroviruses has been highlighted in previous studies using different experimental setups (29, 31, 32). In the case of the human norovirus, recent work using the same replicon in the Huh-7 human hepatoma cell line showed that all three types of IFN, when exogenously added, were able to inhibit HuNoV replication, leading to virus clearance during long-term treatment (34). However, it is not known whether physiological activation of the interferon pathways, particularly the lambda IFN signaling pathway, exerts an antiviral effect against human noroviruses. The present results add further evidence for the involvement of type III IFN in the control of human noroviruses but extend earlier findings, by showing that physiological levels of type III IFN signaling can effectively restrict HuNoV replication. One of the major concerns with replicon systems is that gene expression landscapes might reflect clonal selection of RNA-replicating cells rather than a universal impact of viral replication on cellular gene expression. To exclude the possibility that differences in gene expression were exclusive to a specific cell type or population, we compared our data set with previous genome wide-transcription profiles from Huh-7 hepatoma cells supporting autonomous replication of HuNoV RNAs (44). We found a (significant) positive correlation between the two data sets when statistically differentially expressed genes were compared ( $r = 0.19$ ,  $P = 0.04$ ,  $n = 115$ , or  $r = 0.49$ ,  $P = 0.1$ ,  $n = 12$ , fold change [FC] > 2) (see Tables S6 and S7 in the supplemental material), suggesting that analogous cellular responses were induced in response to HuNoV replication in both cell lines.

It is interesting to note that IFNLR1 mRNA is also downregulated in HGT-NV cells which have not been treated with exogenous type I IFN. This indicates that in the absence of selective pressure mediated by type I IFN, modulation of the type III IFN pathway is preferentially selected over other genes with antiviral properties as exemplified in other studies using RNA replicons with a selectable marker. For example, in the case of HCV replicon systems, several antiviral genes, including *Viperin* and *MX1*, were shown to be silenced through gene methylation, rendering Huh-7 cells permissive to HCV replication (45, 46).

An important observation in this study is the upregulation of several IRF3-dependent genes when HGT-NV cells were compared to parental HGT cells. As IRF3 activation is essential for type I and III interferon induction, upregulation of IRF3-dependent genes suggests that HuNoV replication produces PAMPs that are sensed by RIG-I-like receptor(s), which in turn activates the cell-intrinsic immune signaling pathways. Similarly, downregulation of ISRE-dependent genes in HGT-NV compared to HGT-Cured cells, which have silenced the *IFNLR1* gene to the same extent, put forward the idea that HuNoV replication induces IFN-dependent responses. In line with this, a recent study using the same replicon identified RIG-I and MDA5 proteins as potent negative regulators of HuNoV replication, suggesting that viral RNA secondary structures can readily be detected during replication (34). These observations are, however, in striking contrast to the study by Qu and colleagues in which transfection of stool-derived HuNoV RNA was readily replicated in 293T cells but failed to induce detectable interferon responses (33). Differences in experimental setups including cell lines, virus strains, stable versus transient viral replication, and IFN response readouts may account for this discordant observation. Investigating whether diverse strains of HuNoV induce interferon responses in cell-derived human intestinal enteroids will be of interest to probe the influence of HuNoV replication on IFN induction and responses.

Increased replication of HuNoV in HGT-Cured cells compared to IFNAR and IFNLR1 knockout cells suggests that differentially regulated genes other than IFN receptors may favor virus replication. However, manual curation of genes differentially regulated between parental and IFN-cured cells did not reveal individual genes convincingly known to modulate viral replication other than IFNLR1 and genes involved in the biosynthesis and trafficking of cholesterol. This suggests either that a low but collective

influence of these genes contributes to the increased replication of HuNoV observed in HGT-Cured cells or that some of the differentially expressed genes identified have a potent yet unknown proviral activity toward the human norovirus.

Overall, our results provide insights into the interactions between the human norovirus and innate cellular responses and show that endogenous levels of  $\lambda$ -IFNs control HuNoV replication, suggesting that they may have a therapeutic potential in the treatment of noroviral infections. In addition, the high-confidence gene expression data sets provided with this study are expected to be useful for the selection and examination of new targets for antiviral therapy.

## MATERIALS AND METHODS

**Cells and media.** Human gastric tumor (HGT) cells, human norovirus replicon-harboring HGT (HGT-NV) cells, and IFN- $\alpha$ -treated HGT-NV cells (HGT-Cured) were maintained in Dulbecco's minimal essential medium supplemented with 10% fetal calf serum, 2 mM glutamine, 100 U/ml penicillin, 100  $\mu$ g/ml streptomycin, 1 $\times$  nonessential amino acids, and 0.5 mg/ml G418 in the case of HGT-NV cells. The DNA methyltransferase inhibitor 5-aza-2'-deoxycytidine (Sigma-Aldrich; A3656) was diluted in sterile water and used at a final concentration of 10  $\mu$ M.

**Microarray analysis.** Four lineages of HGT, HGT-NV, and HGT-Cured cells were grown in tissue culture flasks in the appropriate culture medium. After four successive passages, total RNA was extracted using TRIzol (Invitrogen). Microarray analysis was done using the HumanHT-12 v4 Expression BeadChip (Illumina, Chesterford, United Kingdom). All microarray experiments, data normalizations, and preliminary analysis were performed by Cambridge Genomic Services, Cambridge, United Kingdom. To compare changes in gene expression profile between our data set and a previous HuNoV replicon established in Huh-7 hepatoma cells (44), microarray data set [GSE15520](#) from the Gene Expression Omnibus (GEO) database was processed using the GEO2R script and resulting expression profiles were compared using gene names as common identifiers.

**Quantitative RT-PCR analysis.** Total cell RNA was extracted using a GenElute mammalian total RNA miniprep kit (Sigma), and contaminating genomic DNA was removed through RNase-free DNase I treatment (Roche). Total RNA was then reverse transcribed using random hexamers and the Moloney murine leukemia virus (M-MLV) reverse transcriptase (RT) enzyme (Promega). SYBR green-based quantitative PCR was performed using gene-specific primers listed in Table S8 in the supplemental material. Each experimental condition was measured in biological triplicate, and results are shown as a ratio to levels detected in control cells according to the  $\Delta\Delta C_T$  method (47). Additional nontemplate and non-reverse transcriptase samples were analyzed as negative controls. Data were collected using a ViiA 7 real-time PCR system (Applied Biosystems). Genomic viral RNA was quantified by one-step RT-qPCR using GI NV-specific primers. Viral genome copy numbers were calculated by interpolation from a standard curve generated using serial dilutions of viral RNA transcribed from the pNV101 plasmid coding for the full-length Norwalk virus genome (48).

**Nucleic acid transfection and IFN treatment.** Transfections of plasmid DNA or purified viral RNA (NV replicon) were carried out using Lipofectamine 2000 (Invitrogen) according to the manufacturer's instructions. Briefly, cells were seeded in antibiotic-free growth medium at a density of  $2 \times 10^5$  or  $1 \times 10^6$  cells per well in 24- or 6-well plates, respectively, and incubated overnight at 37°C. Lipofectamine 2000 reagent was diluted in Opti-MEM (Gibco) and incubated for 5 min at 25°C. After the incubation, plasmid DNA or viral RNA, diluted in Opti-MEM (Gibco), was mixed with the Lipofectamine–Opti-MEM mixture, vortexed briefly, and incubated at 25°C for 20 min. The DNA or RNA complex was subsequently inoculated onto 80 to 90% confluent cell monolayers, followed by incubation at 37°C. For viral RNA transfection, medium was replaced after 24 h with fresh complete growth medium containing G418 at a concentration of 0.5 mg/ml. For IFN treatments, cells were seeded as described above and incubated at 37°C for indicated time points with or without recombinant type I IFN (IFN- $\beta$ ; Peprtech, catalog no. 300-02BC) or type III IFN (IFN- $\lambda$ 2; Peprtech; catalog no. 300-02K) at a final concentration of 0.1  $\mu$ g/ml.

**Immunofluorescence microscopy.** Cells were plated on 12-mm glass coverslips and allowed to adhere overnight before fixation with 4% paraformaldehyde in phosphate-buffered saline (PBS). Cells were then permeabilized for 5 min with PBS–0.2% Triton X-100, and unspecific antigens were blocked for 1 h using 2% normal goat serum (Sigma; catalog no. S2007) in PBS–0.1% Tween 20 (PBST). Cells were then incubated for 1 h with primary mouse monoclonal J2 anti-dsRNA antibodies in PBST at a dilution of 1:1,000 (J2; Scicons English & Scientific Consulting, Hungary). After extensive washes with PBST, species-matched Alexa Fluor-conjugated secondary antibodies (ThermoFisher Scientific; catalog no. A-11029) were added at a dilution of 1:500 in PBST for 1 additional h. Coverslips were extensively washed and mounted on slides with Mowiol supplemented with 4',6-diamidino-2-phenylindole (DAPI) and 1,4-diazabicyclo(2,2,2)octane (DABCO). Confocal micrographs were acquired on a Leica TCS SP5 confocal microscope fitted with a 63 $\times$  1.3-numerical-aperture (NA) oil immersion objective using 405-nm and 488-nm laser excitation lines under sequential channel scanning to prevent fluorophore bleed-through artifacts due to spectral overlap.

**Western blot analysis.** Cell lysates were prepared in radioimmunoprecipitation assay buffer (RIPA; 150 mM NaCl, 0.5% sodium deoxycholate, 0.1% SDS, 1 mM EDTA, 1% Triton X-100, and 50 mM Tris, pH 8) supplemented with protease and phosphatase inhibitors (Calbiochem; catalog numbers 539134 and 524625). Protein concentrations were determined by bicinchoninic acid (BCA) assay (ThermoFisher

Scientific). Equal amounts of total proteins were resolved by SDS-PAGE and transferred to nitrocellulose membranes. Blocking of unspecific antigens was carried out in 5% nonfat dried milk or 5% bovine serum albumin (BSA) in PBST for 1 h at 4°C. Primary antibodies were diluted in blocking buffer and incubated overnight at 4°C with gentle rocking (Table S8). Membranes were washed three times in PBST for 5 min at room temperature. Species-matched IRDye-800CW secondary antibodies were diluted in blocking buffer as before and incubated at room temperature for 1 h. Membranes were washed again three times in PBST for 5 min at room temperature. Fluorescent signal was detected through an Odyssey CLx infrared imaging system (Li-Cor).

**Generation of IFNAR1- or IFNLR1-knockout HGT cells.** HGT cells knocked out for *IFNAR1* or *IFNLR1* genes were generated using the CRISPR/Cas9 system. Lentivirus vectors carrying single guide RNAs against *IFNAR1* or *IFNLR1* genes were generously provided by Steeve Boulant and are described in the work of Pervolaraki et al. (49). Vesicular stomatitis virus G-protein-pseudotyped lentiviral particles were generated by transient transfection of 293T cells grown in 6-well plates using 1.25 µg lentiviral vector, 0.63 µg pMDLg/pRRE (Addgene number 12251), 0.31 µg pRSV-Rev (Addgene number 12253), and 0.38 µg pMD2.G (Addgene number 12259) per well. Parental HGT cells were transduced with lentiviral supernatants and incubated for 48 h. Transduced cells were then selected on the basis of their resistance to puromycin at a concentration of 2.5 µg/ml. Clonal isolation was performed by limiting dilution into 96-well plates at a density of 0.3 cell per well, and single-cell clones were selected on the basis of visual examination. Single-cell clones were expanded and tested for IFNAR1 or IFNLR1 gene disruption by RT-qPCR measurement of viperin induction following incubation with IFN-β or IFN-λ2, respectively. Absence of STAT1 phosphorylation following incubation with receptor-matched interferons confirmed the gene ablation.

**McrBC cleavage assay.** Two micrograms of genomic DNA extracted from either HGT, HGT-NV, or HGT-Cured cells was digested for 16 h with 10 units McrBC (New England Biolabs) in the presence or absence of GTP. Digested genomic DNA was then purified by ethanol precipitation. Digested DNA was used for PCR amplification analysis using the IFNLR1 promoter-specific primers (IGUC4177, 5'-AGAGGTACGGGCGAGTTTC-3' [Fwd], and IGUC4178, 5'-GACCCGGTTCTGTTCCAGTCC-3' [Rev]) using KOD Hot Start DNA polymerase (Novagen) according to the manufacturer's protocol. PCR products were visualized by electrophoresis on 1% agarose gels run in Tris-borate-EDTA buffer and stained with ethidium bromide.

**Statistical analysis and data sharing.** Statistical significance was determined from experiments where  $n$  was  $\geq 3$  using two-tailed Student  $t$  tests in Prism 6.0 (GraphPad). Asterisks denote the statistical significance of the indicated comparisons as follows: \*,  $P \leq 0.05$ ; \*\*,  $P \leq 0.01$ ; \*\*\*,  $P \leq 0.001$ ; and \*\*\*\*,  $P \leq 0.0001$ . All microarray expression data reported in this study have been deposited into Gene Expression Omnibus (GEO, <https://www.ncbi.nlm.nih.gov/geo>) with the accession number GSE111041.

## SUPPLEMENTAL MATERIAL

Supplemental material for this article may be found at <https://doi.org/10.1128/mBio.02155-19>.

**FIG S1**, PDF file, 0.7 MB.

**FIG S2**, PDF file, 0.8 MB.

**TABLE S1**, XLSX file, 0.04 MB.

**TABLE S2**, XLSX file, 0.9 MB.

**TABLE S3**, XLSX file, 0.8 MB.

**TABLE S4**, XLSX file, 0.1 MB.

**TABLE S5**, XLSX file, 0.1 MB.

**TABLE S6**, XLSX file, 1.4 MB.

**TABLE S7**, XLSX file, 0.05 MB.

**TABLE S8**, XLSX file, 0.04 MB.

## ACKNOWLEDGMENTS

We thank Laure Dumoutier (de Duve Institute, Universite Catholique de Louvain) for the gift of the IFNLR1 (LICR2)-expressing plasmid. We thank K. Green (NIH, Bethesda, MD) and K. O. Chang for the provision of pNV-Neo.

We declare that we have no conflict of interest.

I.G.G. is a Wellcome Senior Fellow, and this work was supported by funding from the Wellcome Trust (reference no. 207498/Z/17/Z). F.S. was funded by a Biotechnology and Biological Sciences Research Council (BBSRC) sLoLa grant (BB/K002465/1). S.A.E. is supported through a Cambridge Trust Cambridge-Africa PhD studentship. The funders had no role in study design, data collection and interpretation, or the decision to submit the work for publication.

S.A.E., F.S., M.H., and I.G.G. designed and performed the research and analyzed the data. S.A.E., F.S., and I.G.G. wrote the manuscript.

## REFERENCES

- Fankhauser RL, Noel JS, Monroe SS, Ando T, Glass RI. 1998. Molecular epidemiology of "Norwalk-like viruses" in outbreaks of gastroenteritis in the United States. *J Infect Dis* 178:1571–1578. <https://doi.org/10.1086/314525>.
- Mawatari M, Kato Y. 2014. Norovirus gastroenteritis, p 203–212. In Ergönül Ö, Can F, Madoff L, Akova M (ed), *Emerging infectious diseases: clinical case studies*. Academic Press, New York, NY. <https://doi.org/10.1016/B978-0-12-416975-3.00016-9>.
- Hall AJ, Lopman BA, Payne DC, Patel MM, Gastañaduy PA, Vinjé J, Parashar UD. 2013. Norovirus disease in the United States. *Emerg Infect Dis* 19:1198–1205. <https://doi.org/10.3201/eid1908.130465>.
- Lopman B, Ahmed SM, Robinson A, Verhoef L, Koopmans M, Hall AJ. 2013. The global prevalence of norovirus among cases of gastroenteritis. *Vaccines for enteritis diseases*, Bangkok, Thailand.
- Ludwig A, Adams O, Laws HJ, Schroten H, Tenenbaum T. 2008. Quantitative detection of norovirus excretion in pediatric patients with cancer and prolonged gastroenteritis and shedding of norovirus. *J Med Virol* 80:1461–1467. <https://doi.org/10.1002/jmv.21217>.
- Patel MM, Widdowson MA, Glass RI, Akazawa K, Vinjé J, Parashar UD. 2008. Systematic literature review of role of noroviruses in sporadic gastroenteritis. *Emerg Infect Dis* 14:1224–1231. <https://doi.org/10.3201/eid1408.071114>.
- Phillips G, Tam CC, Conti S, Rodrigues LC, Brown D, Iturriza-Gomara M, Gray J, Lopman B. 2010. Community incidence of norovirus-associated infectious intestinal disease in England: improved estimates using viral load for norovirus diagnosis. *Am J Epidemiol* 171:1014–1022. <https://doi.org/10.1093/aje/kwq021>.
- Payne DC, Vinjé J, Szilagyi PG, Edwards KM, Staat MA, Weinberg GA, Hall CB, Chappell J, Bernstein DI, Curns AT, Wikswo M, Shirley SH, Hall AJ, Lopman B, Parashar UD. 2013. Norovirus and medically attended gastroenteritis in U.S. children. *N Engl J Med* 368:1121–1130. <https://doi.org/10.1056/NEJMsa1206589>.
- Belliot G, Lopman BA, Ambert-Balay K, Pothier P. 2014. The burden of norovirus gastroenteritis: an important foodborne and healthcare-related infection. *Clin Microbiol Infect* 20:724–730. <https://doi.org/10.1111/1469-0691.12722>.
- Bartsch SM, Lopman BA, Ozawa S, Hall AJ, Lee BY. 2016. Global economic burden of norovirus gastroenteritis. *PLoS One* 11:e0151219. <https://doi.org/10.1371/journal.pone.0151219>.
- Ettayebi K, Crawford SE, Murakami K, Broughman JR, Karandikar U, Tenge VR, Neill FH, Blutt SE, Zeng XL, Qu L, Kou B, Opekun AR, Burrin D, Graham DY, Ramani S, Atmar RL, Estes MK. 2016. Replication of human noroviruses in stem cell-derived human enteroids. *Science* 353:1387–1393. <https://doi.org/10.1126/science.aaf5211>.
- Jones M, Watanabe M, Zhu S, Graves C, Keyes L, Grau K, Gonzalez-Hernandez M, Iovine N, Wobus C, Vinjé J, Tibbetts S, Wallet S, Karst S. 2014. Enteric bacteria promote human and mouse norovirus infection of B cells. *Science* 346:755–759. <https://doi.org/10.1126/science.1257147>.
- Wobus CE, Karst SM, Thackray LB, Chang KO, Sosnovtsev SV, Belliot G, Krug A, Mackenzie JM, Green KY, Virgin HW, IV. 2004. Replication of norovirus in cell culture reveals a tropism for dendritic cells and macrophages. *PLoS Biol* 2:e432. <https://doi.org/10.1371/journal.pbio.0020432>.
- Chang K-O, Sosnovtsev SV, Belliot G, King AD, Green KY. 2006. Stable expression of a Norwalk virus RNA replicon in a human hepatoma cell line. *Virology* 353:463–473. <https://doi.org/10.1016/j.virol.2006.06.006>.
- Thorne LG, Goodfellow IG. 2014. Norovirus gene expression and replication. *J Gen Virol* 95:278–291. <https://doi.org/10.1099/vir.0.059634-0>.
- Isaacs A, Lindenmann J. 1988. Virus interference: I. The interferon. *CA Cancer J Clin* 38:280–290. <https://doi.org/10.3322/canjclin.38.5.280>.
- Kotenko SV, Gallagher G, Baurin VV, Lewis-Antes A, Shen M, Shah NK, Langer JA, Sheikh F, Dickensheets H, Donnelly RP. 2003. IFN- $\lambda$ s mediate antiviral protection through a distinct class II cytokine receptor complex. *Nat Immunol* 4:69. <https://doi.org/10.1038/nri875>.
- Sheppard P, Kindsvogel W, Xu W, Henderson K, Schlutsmeyer S, Whitmore TE, Kuestner R, Garriagues U, Birks C, Roraback J, Ostrander C, Dong D, Shin J, Presnell S, Fox B, Haldeman B, Cooper E, Taft D, Gilbert T, Grant FJ, Tackett M, Krivan W, McKnight G, Clegg C, Foster D, Klucher KM. 2003. IL-28, IL-29 and their class II cytokine receptor IL-28R. *Nat Immunol* 4:63. <https://doi.org/10.1038/nri873>.
- de Weerd NA, Samarajiva SA, Hertzog PJ. 2007. Type I interferon receptors: biochemistry and biological functions. *J Biol Chem* 282:20053–20057. <https://doi.org/10.1074/jbc.R700006200>.
- Sommereyns C, Paul S, Staeheli P, Michiels T. 2008. IFN- $\lambda$  is expressed in a tissue-dependent fashion and primarily acts on epithelial cells in vivo. *PLoS Pathog* 4:e1000017. <https://doi.org/10.1371/journal.ppat.1000017>.
- Blazek K, Eames HL, Weiss M, Byrne AJ, Perocheau D, Pease JE, Doyle S, McCann F, Williams RO, Udalova IA. 2015. IFN- $\lambda$  resolves inflammation via suppression of neutrophil infiltration and IL-1 $\beta$  production. *J Exp Med* 212:845–853. <https://doi.org/10.1084/jem.20140995>.
- Witte K, Gruetz G, Volk HD, Looman AC, Asadullah K, Sterry W, Sabat R, Wolk K. 2009. Despite IFN- $\lambda$  receptor expression, blood immune cells, but not keratinocytes or melanocytes, have an impaired response to type III interferons: implications for therapeutic applications of these cytokines. *Genes Immunity* 10:702–714. <https://doi.org/10.1038/gene.2009.72>.
- Dickensheets H, Sheikh F, Park O, Gao B, Donnelly RP. 2013. Interferon- $\lambda$  induces signal transduction and gene expression in human hepatocytes, but not in lymphocytes or monocytes. *J Leukoc Biol* 93:377–385. <https://doi.org/10.1189/jlb.0812395>.
- Ank N, Iversen MB, Bartholdy C, Staeheli P, Hartmann R, Jensen UB, Dagnaes-Hansen F, Thomsen AR, Chen Z, Haugen H, Klucher K, Paludan SR. 2008. An important role for type III interferon (IFN- $\lambda$ ) in TLR-induced antiviral activity. *J Immunol* 180:2474–2485. <https://doi.org/10.4049/jimmunol.180.4.2474>.
- Syedbasha M, Egli A. 2017. Interferon lambda: modulating immunity in infectious diseases. *Front Immunol* 8:119. <https://doi.org/10.3389/fimmu.2017.00119>.
- Lee S, Baldrige MT. 2017. Interferon-lambda: a potent regulator of intestinal viral infections. *Front Immunol* 8:749. <https://doi.org/10.3389/fimmu.2017.00749>.
- Hemann EA, Gale M, Savan R. 2017. Interferon lambda genetics and biology in regulation of viral control. *Front Immunol* 8:1707. <https://doi.org/10.3389/fimmu.2017.01707>.
- Mordstein M, Neugebauer E, Ditt V, Jessen B, Rieger T, Falcone V, Sorgeloos F, Ehl S, Mayer D, Kochs G, Schwemmler M, Gunther S, Drosten C, Michiels T, Staeheli P. 2010. Lambda interferon renders epithelial cells of the respiratory and gastrointestinal tracts resistant to viral infections. *J Virol* 84:5670–5677. <https://doi.org/10.1128/JVI.00272-10>.
- Baldrige MT, Lee S, Brown JJ, McAllister N, Urbanek K, Dermody TS, Nice TJ, Virgin HW. 2017. Expression of *Irfn1* in intestinal epithelial cells is critical to the antiviral effects of interferon lambda against norovirus and reovirus. *J Virol* 91:e02079-16. <https://doi.org/10.1128/JVI.02079-16>.
- Nice TJ, Baldrige MT, McCune BT, Norman JM, Lazear HM, Artyomov M, Diamond MS, Virgin HW. 2015. Interferon- $\lambda$  cures persistent murine norovirus infection in the absence of adaptive immunity. *Science* 347:269–273. <https://doi.org/10.1126/science.1258100>.
- Baldrige MT, Nice TJ, McCune BT, Yokoyama CC, Kambal A, Wheadon M, Diamond MS, Ivanova Y, Artyomov M, Virgin HW. 2015. Commensal microbes and interferon-lambda determine persistence of enteric murine norovirus infection. *Science* 347:266–269. <https://doi.org/10.1126/science.1258025>.
- Rocha-Pereira J, Jacobs S, Noppen S, Verbeke E, Michiels T, Neyts J. 2018. Interferon lambda (IFN- $\lambda$ ) efficiently blocks norovirus transmission in a mouse model. *Antiviral Res* 149:7–15. <https://doi.org/10.1016/j.antiviral.2017.10.017>.
- Qu L, Murakami K, Broughman JR, Lay MK, Guix S, Tenge VR, Atmar RL, Estes MK. 2016. Replication of human norovirus RNA in mammalian cells reveals lack of interferon response. *J Virol* 90:8906–8923. <https://doi.org/10.1128/JVI.01425-16>.
- Dang W, Xu L, Yin Y, Chen S, Wang W, Hakim MS, Chang KO, Peppelenbosch MP, Pan Q. 2018. IRF-1, RIG-I and MDA5 display potent antiviral activities against norovirus coordinately induced by different types of interferons. *Antiviral Res* 155:48–59. <https://doi.org/10.1016/j.antiviral.2018.05.004>.
- Arthur SE, Sorgeloos F, Hosmillo M, Goodfellow I. 2019. Epigenetic suppression of interferon lambda receptor expression leads to an enhanced HuNoV replication in vitro. *bioRxiv* 523282.
- Weber F, Wagner V, Rasmussen SB, Hartmann R, Paludan SR. 2006. Double-stranded RNA is produced by positive-strand RNA viruses and DNA viruses but not in detectable amounts by negative-strand RNA

- viruses. *J Virol* 80:5059–5064. <https://doi.org/10.1128/JVI.80.10.5059-5064.2006>.
37. Son K-N, Liang Z, Lipton HL. 2015. Double-stranded RNA is detected by immunofluorescence analysis in RNA and DNA virus infections, including those by negative-stranded RNA viruses. *J Virol* 89:9383–9392. <https://doi.org/10.1128/JVI.01299-15>.
  38. Andersen J, VanScoy S, Cheng TF, Gomez D, Reich NC. 2008. IRF-3-dependent and augmented target genes during viral infection. *Genes Immun* 9:168–175. <https://doi.org/10.1038/sj.gene.6364449>.
  39. Grandvaux N, Servant MJ, tenOever B, Sen GC, Balachandran S, Barber GN, Lin R, Hiscott J. 2002. Transcriptional profiling of interferon regulatory factor 3 target genes: direct involvement in the regulation of interferon-stimulated genes. *J Virol* 76:5532–5539. <https://doi.org/10.1128/JVI.76.11.5532-5539.2002>.
  40. Friedman RL, Manly SP, McMahon M, Kerr IM, Stark GR. 1984. Transcriptional and posttranscriptional regulation of interferon-induced gene expression in human cells. *Cell* 38:745–755. [https://doi.org/10.1016/0092-8674\(84\)90270-8](https://doi.org/10.1016/0092-8674(84)90270-8).
  41. Reid LE, Brasnett AH, Gilbert CS, Porter AC, Gewert DR, Stark GR, Kerr IM. 1989. A single DNA response element can confer inducibility by both alpha- and gamma-interferons. *Proc Natl Acad Sci U S A* 86:840–844. <https://doi.org/10.1073/pnas.86.3.840>.
  42. Odendall C, Dixit E, Stavru F, Bierne H, Franz KM, Durbin AF, Boulant S, Gehrke L, Cossart P, Kagan JC. 2014. Diverse intracellular pathogens activate type III interferon expression from peroxisomes. *Nat Immunol* 15:717–726. <https://doi.org/10.1038/ni.2915>.
  43. Ding S, Khoury-Hanold W, Iwasaki A, Robek MD. 2014. Epigenetic reprogramming of the type III interferon response potentiates antiviral activity and suppresses tumor growth. *PLoS Biol* 12:e1001758. <https://doi.org/10.1371/journal.pbio.1001758>.
  44. Chang K-O. 2009. Role of cholesterol pathways in norovirus replication. *J Virol* 83:8587–8595. <https://doi.org/10.1128/JVI.00005-09>.
  45. Naka K, Abe K, Takemoto K, Dansako H, Ikeda M, Shimotohno K, Kato N. 2006. Epigenetic silencing of interferon-inducible genes is implicated in interferon resistance of hepatitis C virus replicon-harboring cells. *J Hepatol* 44:869–878. <https://doi.org/10.1016/j.jhep.2006.01.030>.
  46. Chen Q, Denard B, Huang H, Ye J. 2013. Epigenetic silencing of antiviral genes renders clones of Huh-7 cells permissive for hepatitis C virus replication. *J Virol* 87:659–665. <https://doi.org/10.1128/JVI.01984-12>.
  47. Schmittgen TD, Livak KJ. 2008. Analyzing real-time PCR data by the comparative CT method. *Nat Protoc* 3:1101–1108. <https://doi.org/10.1038/nprot.2008.73>.
  48. Fernandez-Vega V, Sosnovtsev SV, Belliot G, King AD, Mitra T, Gorbalenya A, Green KY. 2004. Norwalk virus N-terminal nonstructural protein is associated with disassembly of the Golgi complex in transfected cells. *J Virol* 78:4827–4837. <https://doi.org/10.1128/JVI.78.9.4827-4837.2004>.
  49. Pervolaraki K, Stanifer ML, Münchau S, Renn LA, Albrecht D, Kurzhals S, Senís E, Grimm D, Schröder-Braunstein J, Rabin RL, Boulant S. 2017. Type I and type III interferons display different dependency on mitogen-activated protein kinases to mount an antiviral state in the human gut. *Front Immunol* 8:459. <https://doi.org/10.3389/fimmu.2017.00459>.